JPET Fast Forward. Published on March 22, 2005 as DOI: 10.1124/jpet.104.082826
JPET#82826

CYP3A4 SUBSTRATE SELECTION AND SUBSTITUTION IN THE PREDICTION OF POTENTIAL DRUG-DRUG INTERACTION

Aleksandra Galetin, Kiyomi, Ito, David Hallifax and J. Brian Houston

School of Pharmacy and Pharmaceutical Sciences, University of Manchester, Oxford Road, Manchester, M13 9PL, United Kingdom (A.G., D.H. and J.B.H.) and Department of Clinical Pharmacokinetics, Hoshi University, Tokyo, Japan (K.I.)

JPET Fast Forward. Published on March 22, 2005 as DOI: 10.1124/jpet.104.082826
This article has not been copyedited and formatted. The final version may differ from this version.

a) Running title: CYP3A4 substrate substitution in drug interaction prediction

b) **Corresponding author:** Dr A. Galetin

School of Pharmacy and Pharmaceutical Sciences,

University of Manchester,

Oxford Road,

Manchester, M13 9PL, UK

Tel: (+) 44 161 275 6886

Fax: (+) 44 161 275 8349

Email: Aleksandra.Galetin@manchester.ac.uk

c) Text: 40

Tables: 2

Figures: 5

References: 40

Abstract: 242

Introduction: 749

Discussion: 1,416

d) **Abbreviations used are:** DDI, drug-drug interactions; γ, interaction factor for the change in catalytic rate constant; δ interaction factor for the change in binding affinity (heterotropic cooperativity); rmse, root mean squared prediction error.

e) Absorption, Distribution, Metabolism and Excretion

JPET Fast Forward. Published on March 22, 2005 as DOI: 10.1124/jpet.104.082826
This article has not been copyedited and formatted. The final version may differ from this version.

ABSTRACT

The complexity of in vitro kinetic phenomena observed for CYP3A4 substrates (homo- or heterotropic cooperativity) confounds the prediction of drug-drug interactions and an evaluation of alternative and/or pragmatic approaches and substrates is needed. The current study focused on the utility of the three most commonly used CYP3A4 in vitro probes for the prediction of 26 reported in vivo interactions with azole inhibitors (increase in AUC ranged from 1.2-24, 50% in the range of potent inhibition). In addition to midazolam, testosterone and nifedipine, quinidine was explored as a more 'pragmatic' substrate due to its kinetic properties and specificity towards CYP3A4 in comparison to CYP3A5. K_i estimates obtained in human liver microsomes under standardised in vitro conditions for each of the four probes were used to determine the validity of substrate substitution in CYP3A4 drug-drug interaction prediction. Detailed inhibitor-related (microsomal binding, depletion over incubation time) and substrate-related factors (cooperativity, contribution of other metabolic pathways or renal excretion) were incorporated in the assessment of the interaction potential. All four CYP3A4 probes predicted 69-81% of the interactions with azoles within 2-fold of the mean in vivo value. Comparison of simple and multisite mechanistic models and interaction prediction accuracy for each of the in vitro probes, indicated that midazolam and quinidine in vitro data provided the best assessment of a potential interaction, with the lowest bias and the highest precision of the prediction. Further investigations with a wider range of inhibitors are required to substantiate these findings.

CYP3A4 is the most abundant human P450 enzyme metabolizing a wide range of structurally diverse therapeutic agents, hence it is the target for many drug-drug interactions (DDI). A recent FDA report (Yuan et al., 2002) has shown testosterone to be the most commonly used in vitro CYP3A4 probe (50% of reported studies) in contrast to midazolam (15-20% of in vitro estimates of CYP3A4 activity) whereas nifedipine, felodipine and erythromycin were employed in less than 10% of studies. The existence of different substrate subgroups for CYP3A4 was based on correlation and cluster analysis of CYP3A4 inhibition data for a range of modifiers (Kenworthy et al., 1999). This was substantiated by others (Stresser et al., 2000) and further investigated in a number of detailed mechanistic kinetic studies (Houston et al., 2003) that indicated the existence of distinct and preferential binding domains for each substrate subgroup, namely midazolam, testosterone and nifedipine. Due to the substrate-differential response observed for CYP3A4, the recommended approach to CYP3A4 DDI analysis is the use of multiprobes (Tucker et al., 2001; Bjornsson et al., 2003) where the lowest inhibition constant (K_i) obtained indicates the 'worst case scenario' for a potential interaction. However, an inappropriate selection of a probe substrate may lead to false positive or negative prediction of a DDI.

An additional complicating issue in the assessment of CYP3A inhibition potential is the occurrence of homo/heterotropic cooperativity in vitro. This may result in a sigmoidal kinetic profile (for testosterone), substrate inhibition (for nifedipine) and limited substrate substitution and inhibitory reciprocity (Korzekwa, 2002; Houston et al., 2003). These 'atypical' phenomena attributed to the existence of multiple binding sites have been associated with CYP3A4; however recent studies indicate similar behaviour for other CYP (Egnell et al., 2003, Hutzler et al., 2003) and UGT enzymes (Uchaipichat et al., 2003). The incorporation of homo/heterotropic

cooperativity in the in vitro-in vivo prediction of either clearance or DDI is not widely adopted. While their actual in vivo relevance remains questionable, appropriate in vitro analysis is essential for accurate quantitative estimates of both clearance and DDI (Houston and Galetin, 2003).

In order to provide a link between the in vitro multisite inhibition data and the actual in vivo inhibition interactions, a prediction equation based on the same rapid equilibrium /steady state assumptions as the single-site inhibition models (Segel, 1975) has been derived (Appendix). In accordance with previous analysis (Tucker et al., 2001, Ito et al., 2004), the metric for the degree of DDI is the AUCi/AUC ratio for the plasma concentration-time profiles in the presence and absence of the inhibitor, respectively. The complexity of multisite kinetic analysis observed with certain CYP3A4 substrates indicated the need for an assessment of alternative and/or more pragmatic approaches and substrates for the prediction of potential DDI involving this enzyme.

The aim of the current study was to evaluate the importance of substrate selection for predicting a range of reported CYP3A4 drug interactions with the ketoconazole, itraconazole and fluconazole. The in vivo interactions previously reported by Ito et al. (2004) were critically reviewed and 26 studies were selected, including 13 different CYP3A4 substrates from different therapeutic and substrate-subgroups. Classifying these studies according to Bjornsson et al. (2003) (Fig. 1) indicated that 50% of interactions were in the range of potent inhibition (AUCi/AUC >5) .

The importance of substrate selection (and/or appropriate substitution) was assessed by comparing the extent of predicted AUCi/AUC ratios for a range of CYP3A4 in vivo interactions applying the K_i estimates for either midazolam,

testosterone, nifedipine or quinidine. In addition to the three most commonly used in vitro probes, quinidine was investigated as a 'pragmatic' substrate due to its apparent Michaelis-Menten kinetic properties and specificity towards CYP3A4 in comparison to CYP3A5 (Galetin et al., 2004). In order to minimise experimental variability and provide the least bias in the in vitro estimates, all the inhibition studies were performed under standardised conditions using the same batch of human liver microsomes, low protein concentration and an appropriate range of concentrations for both the inhibitor and substrate. Detailed inhibitor- (microsomal binding, depletion over incubation time) and substrate-related factors (cooperativity, contribution of other metabolic pathways or renal excretion) were incorporated in the prediction of DDI.

The current study demonstrates that the 'simple' in vitro inhibition profiles of midazolam and quinidine with azoles provide good DDI prediction accuracy and precision. In comparison to other probes (nifedipine and testosterone), they offer a more pragmatic choice of substrate for extrapolation across the range of CYP3A substrates and identification of potential DDI from in vitro data.

Materials and Methods

Chemicals. Midazolam, testosterone, quinidine, nifedipine, 6β-hydroxytestosterone, ketoconazole, fluconazole, prednisone, verapamil, dextromethorphan, NADP, isocitric dehydrogenase were purchased from Sigma Chemicals Co. (Poole, Dorset, UK). (3S)-3-hydroxyquinidine, oxidized nifedipine, itraconazole and midazolam metabolites were obtained from Ultrafine Chemicals (Manchester, UK). All other reagents and solvents were of high analytical grade. Pooled human liver microsomes (n=22, testosterone 6β-hydroxylation activity =6.4 nmol/min/mg protein) were obtained from BD Gentest Co. (Woburn, MA, USA).

In vitro inhibition studies. Interaction studies were performed at incubation times (2.5 min – midazolam, 10 min – nifedipine and 15 min quinidine and testosterone) and protein concentrations (0.25 mg/ml) were within the linear range for the each substrate. Microsomes were suspended in phosphate buffer (0.1 M, pH 7.4) with the final incubation volume of 0.25 mL. Samples were pre-incubated for 5 min in a shaking water bath at 37°C and each reaction was initiated with an NADPH regenerating system (1mM $NADP^+$, 7.5 mM isocitric acid, 10 mM magnesium chloride and 0.2 units isocitric dehydrogenase). The final concentration of the organic solvent (either methanol or acetonitrile) in incubation media was 0.2 % v/v. The substrate concentrations ranged from.5-50 μM (midazolam), 25-250 μM (quinidine), 2.5-100 μM (nifedipine) and 5-200 μM (testosterone). The concentrations of the inhibitors ranged from 0.01-10 μM (ketoconazole), 0.1-100 μM (fluconazole) and 0.01-10 μM (itraconazole). The reaction was terminated by 0.25 mL of ice-cold acetonitrile with 1μM of the appropriate internal standard, samples were centrifuged at 13,400g for 10 min and further analyzed by LC-MS/MS.

Microsomal binding and inhibitor depletion. In addition to the effect of multisite binding on K_i estimates, the impact of non-specific microsomal binding and depletion of an inhibitor during the incubation time on the K_i estimates was assessed. Depletion of azoles was evaluated over the range of substrate concentrations investigated (above and below K_m) for each individual substrate.

Binding to microsomes. The binding of the inhibitors to human liver microsomes was determined by either microfiltration or dialysis, depending upon the extent of non-specific binding to microfiltration tubes. Fluconazole was incubated (nominally 1 and 10 μM) with microsomes (0.5, 1.0 or 2.0 mg protein/ml) in 0.1 M phosphate buffer (0.5 ml, including 1% acetonitrile from the dilution of fluconazole) at 37 ^{o}C for 10 min. The incubate was filtered by centrifugation at about 10,000 *g* for 10 s through Whatman Anopore 0.05 μ microfiltration tubes (Whatman, Maidstone, UK). Samples of the incubate and filtrate were analysed by LC-MS/MS. The binding of ketoconazole and itraconazole was determined by dialysis. Cellulose membranes (Dianorm, Munich, Germany) were conditioned overnight in 0.1 M phosphate buffer, at about 10 ^{o}C. The compounds were incubated (nominally at 1 μM) with microsomes (0.01, 0.03, 0.1, and 0.5 mg protein/ml) in 0.1 M phosphate buffer (1.0 ml, including 1% acetonitrile from the dilution of ketoconazole or itraconazole) contained in Dianorm dialysis chambers which were rotated at 37 ^{o}C for 6 h. Samples of dialysate were collected at 1, 3 and 6 h and analysed, together with samples of the solution added to the microsomes, by LC-MS/MS.

Determination of substrate and metabolite concentration. The metabolites 1′-hydroxymidazolam, 3-hydroxyquinidine, oxidized nifedipine, 6β-hydroxytestosterone and the inhibitors ketoconazole, fluconazole and itraconazole were quantified by LC-MS/MS. For each assay, nine calibration standards with a

blank were prepared in a matrix identical to the incubation extracts and included levels at below and above the expected concentrations. Each metabolite, together with either alprazolam (1'-hydroxymidazolam), dextromethorphan (3-hydroxyquinidine, oxidized nifedipine), or prednisone (6β-hydroxytestosterone) as internal standard and either inhibitor (with verapamil as internal standard), were separated on a Luna C18(2) 50 x 4.6 mm 3 µm column (Phenomenex, UK) at 40 °C using either a binary or ternary gradient maintained at 1 ml/min by a Waters Alliance 2795 HT LC system.

For 1'-hydroxymidazolam/fluconazole/ketoconazole, an initial mobile phase of 90 % 0.001 M ammonium acetate/ 10 % acetonitrile was ramped immediately to 29 % 0.001 M ammonium acetate/ 42 % acetonitrile/ 29 % formic acid at 1 minute and immediately to 34 % 0.001 M ammonium acetate/ 66 % acetonitrile at 4 minutes. The initial ratio was immediately re-established at 5 minutes and maintained to 6 minutes. For 1'-hydroxymidazolam/itraconazole, an initial mobile phase of 90 % 0.001 M ammonium acetate/ 10 % acetonitrile was ramped linearly to 10 % 0.001 M ammonium acetate/ 90 % acetonitrile between 1 and 5 minutes and maintained for 1 minute. The initial ratio was immediately re-established at 6 minutes and maintained to 7 minutes.

For 3-hydroxyquinidine/fluconazole/ketoconazole, an initial mobile phase of 90 % 0.001 M ammonium acetate/ 10 % acetonitrile was ramped linearly to 90 % 0.01 M formic acid/ 10 % acetonitrile between 1 and 4 minutes. The initial ratio was immediately re-established at 4 minutes and maintained to 5 minutes. For 3-hydroxyquinidine/itraconazole, an initial mobile phase of 90 % 0.001 M ammonium acetate/ 10 % acetonitrile was ramped linearly to 58 % 0.01 M formic acid/ 42 % acetonitrile between 1 and 3 minutes and immediately to 10 % 0.01 M formic acid/ 90

% acetonitrile at 3 minutes. The initial ratio was immediately re-established at 4 minutes and maintained to 5 minutes.

For oxidized nifedipine/fluconazole/ketoconazole/itraconazole, an initial mobile phase of 74 % 0.01 M formic acid/ 26 % acetonitrile was ramped linearly to 10 % 0.01 M formic acid / 90 % acetonitrile between 1 and 3 minutes and maintained to 4 minutes. The initial ratio was immediately re-established at 4 minutes and maintained to 5 minutes.

For 6β-hydroxytestosterone/fluconazole/ketoconazole, an initial mobile phase of 90 % 0.01 M formic acid/ 10 % acetonitrile was ramped linearly to 54 % 0.01 M formic acid / 46 % acetonitrile between 1 and 3 minutes and immediately to 10 % 0.01 M formic acid/ 90 % acetonitrile at 3 minutes. The initial ratio was immediately re-established at 4 minutes and maintained to 5 minutes. For 6β-hydroxytestosterone/itraconazole, an initial mobile phase of 90 % 0.01 M formic acid/ 10 % acetonitrile was ramped linearly to 10 % 0.01 M formic acid / 90 % acetonitrile between 1 and 4 minutes. The initial ratio was immediately re-established at 4 minutes and maintained to 5.5 minutes.

For fluconazole, ketoconazole and itraconazole, an initial mobile phase of 90 % 0.01 M formic acid/ 10 % acetonitrile was ramped linearly to 10 % 0.01 M formic acid / 90 % acetonitrile between 1 and 3 minutes and maintained to 4 minutes. The initial ratio was immediately re-established at 4 minutes and maintained to 5 minutes.

The compounds were detected and quantified by atmospheric pressure electrospray ionisation MS/MS using a Micromass Quattro Ultima triple quadrupole mass spectrometer. The LC column eluate was split and ¼ was delivered into the MS where the desolvation gas (nitrogen) flow rate was 600 l/hr, the cone gas (nitrogen)

flow rate was 100 l/hr or 300 l/hr (6β-hydroxytestosterone only) and the source temperature was 125 °C.

Using positive ion mode, protonated molecular ions were formed using a capillary energy of 3.5 kV and cone energies of 36 V (ketoconazole), 56 V (fluconazole), 60 V (prednisone, verapamil), 70 V (6β-hydroxytestosterone, 3-hydroxyquinidine, oxidized nifedipine, alprazolam), 79 V (itraconazole), 80 V (1'-hydroxymidazolam) and 89 V (dextromethorphan). Product ions formed in argon at a pressure of 2 $x10^{-3}$ mbar and at collision energies of 10 eV (prednisone, m/z 359.35→341.0), 15 eV (6β-hydroxytestosterone, m/z 305.35→269.0), 17 eV (fluconazole, m/z 307.0→220.0), 20 eV (oxidized nifedipine, m/z 345.0→284.0), 23 eV (3-hydroxyquinidine, m/z 341.15→226.0), 25 eV (alprazolam, m/z 309.05→281.0), 30 eV (1'-hydroxymidazolam, m/z 342.05→203.0; ketoconazole, m/z 531.05→489.0; verapamil, m/z 455.2→165.0) and 40 eV (dextromethorphan, 272.1→170.8; ICZ, m/z 705.0→392.0) were monitored as ion chromatograms which were integrated and quantified by quadratic regression analysis of standard curves using Micromass QuanLynx 3.5 software.

The accuracy of the method was assumed to be adequate as the concentrations were calculated from calibration standards prepared in the same way as the extracts (spike calibration). Values were accepted if the internal standard ratio was greater than a value equal to the calibration regression intercept plus approximately 10 times the estimated standard deviation of the intercept (LLOQ). Repeatability precision was considered adequate if duplicate sample values were within 10% of each other.

Analysis of Multisite Inhibition Data. The kinetic parameters were calculated from untransformed data by nonlinear least squares regression using GraFit 5 (Erithacus Software, Horley, Surrey, UK). The changes in kinetic parameters

observed in the presence of various modifiers were significance tested using analysis of variance. For all four sets of data, analysis was based on the application of simple one-site or multisite kinetic models. According to the kinetic properties of the substrate, variations of the generic two-site model (Galetin et al, 2002) were applied to rationalize the inhibition profiles obtained for midazolam, quinidine and nifedipine. These two-site kinetic models accommodated alterations in binding affinity (δ) and catalytic efficiency upon effector binding (γ). In addition, in case of nifedipine interactions the two-site kinetic model incorporated the substrate inhibition phenomenon defined by the decrease in product formation (K_p) from SES by the factor β (<1). In contrast, the three-site kinetic model was applied for testosterone interactions as positive cooperative binding of testosterone molecules was unaffected by increasing inhibitor concentration, indicating that the inhibitor acts at a distinct effector site. The two- and three-site kinetic models applied and the corresponding equations with the interaction factors were defined in our previous publications (Galetin et al., 2003, Houston and Galetin, 2005). Goodness of fit was determined by visual inspection of the fits, comparison of statistical parameters (χ^2 and Akaike information criterion values) between the models and a reduction in the standard errors of the parameter estimates.

DDI Prediction. In vivo studies used as a comparator have been selected from a database previously collated in our laboratory (Ito et al., 2004a, b). In the case of replicate studies (same dose of the inhibitor, see Table 2) the weighted mean of the AUC ratios was obtained for further analysis. In all the studies AUC (0-∞) was used for this purpose, the only exception was the ketoconazole and itraconazole interaction with triazolam (Varhe et al., 1994) where the AUC at the last time point was used. Whenever available, the mean ± sd estimates of the AUCi/AUC ratio (Fig. 1) were

estimated from the individual AUC values reported in vivo; otherwise the sd values were obtained using equation 1, assuming the normal distribution of the data (Armitage et al., 1985):

$$var(Y) = sd(Y)^2 = var(X_1)/(X_2)^2 + ((X_1)^2/(X_2)^4) * var(X_2) \quad (1)$$

where Y represents the mean AUC ratio, X_1 and X_2 are mean AUC values in the presence and absence of the inhibitor, respectively and $varX_1$ and $varX_2$ represent their respective variances ($var = sd^2$).

The success of AUCi/AUC ratio prediction for 26 reported CYP3A4 in vivo interactions applying either the K_i estimates for midazolam, testosterone, nifedipine or quinidine was assessed. For cases when the two-site model was used to obtain the K_i value (e.g. nifedipine), corresponding two-site equation (Eq. 2) was applied in the prediction. In addition to $[I]/K_i$ ratio, this two-site model equation also incorporates changes in the catalytic efficacy (γ) and binding affinity (δ) in the presence of the inhibitor (See Appendix). In cases when $\gamma/\delta = 1$ two-site prediction equation is reduced to the simple $1+[I]/K_i$ relationship.

$$AUCi/AUC = \frac{\left(1+\frac{[I]}{K_i}\right)^2}{1+\frac{\gamma[I]}{\delta K_i}} \quad (2)$$

where I represents the in vivo inhibitor concentration (either [I]in – input plasma concentration or [I]av – average plasma concentration during the dosing interval (values taken from Ito et al., 2004), whereas K_i estimates are obtained applying the generic two-site model (Houston and Galetin, 2003). When one- or three-site models are applied for the analysis of in vitro data, DDI prediction equation involving the

JPET Fast Forward. Published on March 22, 2005 as DOI: 10.1124/jpet.104.082826
This article has not been copyedited and formatted. The final version may differ from this version.

interaction factors is not necessary and the simple $1+[I]/K_i$ relationship is adequate (See Appendix, Eq. 12).

Range of the predicted AUC ratios was obtained by Monte Carlo simulations (Nestorov et al., 2001) applying $[I]av/K_{i,u}$ (inhibitor concentrations taken from the in vivo database, Ito et al., 2004). Contribution of parallel pathways (i.e., other CYP enzymes or renal clearance) was assessed by incorporating the fm values reported by Brown et al. (submitted for publication), using the following equation (Rowland and Matin, 1973):

$$\text{AUCi/AUC} = \frac{1}{\frac{\text{fm}}{1+[\text{I}]/\text{Ki}} + (1-\text{fm})} \quad (3)$$

The bias of DDI prediction was assessed from the geometric mean of the ratio of predicted and actual value (average-fold error - *afe*). The mean squared prediction error (*mse*) (difference between the predicted and observed in vivo value) and the root mean squared prediction error (*rmse*) provided a measure of precision for the prediction of 26 in vivo DDI using midazolam, testosterone, nifedipine and quinidine (Sheiner and Beal, 1981; Obach et al., 1997):

$$afe = 10^{\left|\frac{1}{n}\sum \log\frac{\Pr edicted}{Observed}\right|} \quad (4)$$

$$mse = \frac{1}{n}\sum\left(\Pr edicted - Observed\right)^2 \quad (5)$$

$$rmse = \sqrt{mse} \quad (6)$$

Out of the three itraconazole metabolites reported by Isoherranen et al. (2004) (hydroxy-, keto- and N-desalkyl-itraconazole) only the contribution of hydroxy-itraconazole was included in the prediction. The contribution of the active metabolite (hydroxy-itraconazole) was incorporated as $[1+[I]av/K_{i,u})_{itraconazole} + ([I]av/K_{i,u})_{hydroxy\text{-}itraconazole}]$, where I and K_i values for the metabolite are literature values (Ito et al.,

2004). Microsomal binding was assumed to be the same for the metabolite as determined for the parent.

Results

K_i estimation for azole inhibitors. The inhibitory potency rank order (ketoconazole > itraconazole > fluconazole) was the same for each of the four substrates. Overall, the most potent inhibition was observed when midazolam and quinidine were used as probes, whereas K_i values for nifedipine were 7 to 13-fold higher than values obtained for other CYP3A4 substrates (Table 1). A similar trend in K_i values (midazolam generating the lowest K_i) was observed with a wider range of inhibitors (nifedipine, felodipine, verapamil, diltiazem, saquinavir, data not shown).

In all substrate incubations ketoconazole and itraconazole concentrations were depleted less than 20% over the incubation times applied, whereas no depletion was observed for fluconazole. The trend observed was constant across the substrate concentration range investigated and was greatest at higher concentrations of the inhibitor; hence no corrections in K_i estimates were incorporated. Corrections for microsomal binding were applied for ketoconazole and itraconazole K_i values, with microsomal fraction unbound values of 0.71 and 0.056, respectively at the protein concentration used in the study (0.25 mg/mL), whereas no correction was made for fluconazole (microsomal fraction unbound 0.95).

Significance of multisite modelling approach for azoles interactions. K_i estimates for midazolam, quinidine, testosterone and nifedipine were obtained using both single site (competitive or non-competitive) and multisite inhibition models (either two- or three-site) (Galetin et al., 2002).

For interactions with midazolam and quinidine (Fig. 3A and B, respectively) non-competitive and competitive inhibition models, respectively gave comparable K_i estimates to the generic two-site kinetic model (e.g., ketoconazole-midazolam - 0.06

and 0.07 μM, respectively). In addition, the two-site kinetic analysis of these interactions generated γ/δ ratio values close to 1 (0.9-1.1).

In the case of testosterone all azoles caused changes in the rate of product formation rather than the binding affinity and did not alter the cooperative binding of testosterone molecules (Fig. 3C). The three-site model applied for the analysis of the multisite inhibition interactions with azoles was the same as described previously for the effect of progesterone and quinidine on this CYP3A4 substrate (Galetin et al., 2002). However, the binding affinity of azoles inhibitors was significantly higher (Houston and Galetin, 2005) and the non-productive complexes (SEI, SESI) are formed at lower concentrations of the modifier in contrast to quinidine and progesterone. One-site inhibition models provided a poor fit that showed no agreement with the data observed, particularly at low substrate concentrations, where positive cooperative behaviour was evident.

Nifedipine is a prototypical substrate reported to show negative homotropy; therefore a two-site kinetic model with substrate inhibition was applied for the analysis of its interaction data (Galetin et al., 2003). A 3-fold range in the γ/δ ratio was observed for the three azoles (Fig. 2), mainly as a result of their effect on the rate of product formation (γ), as similar changes in the binding affinity (defined by δ = 0.11-0.14) were observed. In contrast to midazolam and quinidine, a non-competitive inhibition model was not adequate, resulting in a significant difference in K_i values obtained (3 to 12.4-fold). Figure 3D illustrates the relationship between K_i, dissociation constant (K_s) and the interaction factors defining product formation from SES and ISE (βK_p and γK_p, respectively) on the maintenance of negative cooperativity in the presence of the modifier. In cases when γ is comparable to β and $K_i < K_s$ (up to ten-fold, e.g., itraconazole, Figure 3D) or $K_i > K_s$ (e.g., fluconazole-nifedipine, data

not shown), substrate inhibition is maintained at low concentrations of the modifier . However, if K_i <<K_s (e.g. 50-100-fold), the complex with the modifier (ISE) is rapidly formed and no substrate inhibition is noted even at very low inhibitor concentrations (example not shown).

Assessment of DDI potential. The AUC increase in the presence of ketoconazole ranged from 1.2 for tacrolimus to 24-fold for nisoldipine (Table 2). In vivo the effect of itraconazole showed a 19-fold difference among 12 studies, whereas a 2.7-fold range was observed for fluconazole (6 studies). The utility of each of the four CYP3A4 probes for predicting drug-drug interactions via the AUC ratio was investigated using 26 selected CYP3A4 in vivo interactions. The AUC ratios were predicted by Monte Carlo simulations applying $[I]av/K_{i,u}$ (Houston and Galetin, 2005) and the mean values obtained are presented in Table 2. For each correlation set (Fig. 4A-D) the K_i values for only one substrate were employed, i.e., midazolam testosterone, nifedipine and quinidine, respectively. The fm values for the corresponding substrates involved in the in vivo interaction were used (Brown et al., submitted for publication) and are listed in Table 2.

Evaluation of midazolam as a probe. Of the 26 interactions investigated, 77% of AUCi/AUC ratios predicted from K_i estimates using midazolam as a probe were within the 2-fold range of the in vivo value (Fig. 4A). Midazolam successfully predicted the interactions with all benzodiazepines, in contrast to testosterone where 71% of the interactions were within 2-fold (Fig. 5). Incorporation of the fm values for quinidine, alprazolam and cerivastatin (0.76, 0.8 and 0.37, respectively) reduced the over-prediction of the interactions with these substrates by 2.6, 3.8 and 5.2-fold, respectively whereas the impact of such information was of less significance for other substrates (fm range 0.9-0.99).

Evaluation of testosterone as a probe. Testosterone K_i values predicted interactions with cyclosporine within 2-fold of in vivo value, whereas other probes over-estimated the degree of interaction with cyclosporine up to 4-fold. In contrast to midazolam, testosterone under-predicted 29% of reported studies with benzodiazepines. These findings were consistent with substrate substitution within the same CYP3A4 substrate subgroup (Houston and Galetin, 2005). Out of 26 interactions investigated, 69% of AUC ratios predicted were within a 2-fold range of the in vivo value, whereas under-prediction was observed in 6/26 studies (Fig. 4B). The extent of over-prediction was reduced 5 to 12-fold for alprazolam and cerivastatin, respectively when the contribution of the renal clearance and metabolism via CYP2C8, respectively were included in the prediction.

Evaluation of quinidine and nifedipine as probes. AUC ratios predicted using quinidine K_i values were comparable to midazolam predictions as 81% of the estimates were within 2-fold of the observed in vivo value. Use of quinidine provided low bias and the highest precision of the DDI prediction (rmse 4 to 10-fold lower compared to the other three substrates). Among the probe substrates assessed, only quinidine estimated the degree of interaction between ketoconazole and tacrolimus accurately (5.4 to 13-fold over-estimation using testosterone and nifedipine K_i values, respectively). Predicted AUCi/AUC ratios from quinidine in vitro data (Table 2) showed a statistically significant correlation (Pearson correlation coefficient of 0.98, $p<0.05$) with both midazolam and nifedipine, whereas no such relationship could be established with other pairs of probes (Pearson correlation coefficient <0.6, $p>0.1$).

Success in prediction using nifedipine K_i values was comparable to testosterone (69% of mean AUC ratios predicted within the 2-fold range), with under-prediction observed in 6/26 studies (maximum of 5-fold in case of itraconazole-

lovastatin). The two-site prediction approach reduced the average-fold error by half and improved the precision of the DDI assessment (rmse reduced by 80%) in comparison to non-competitive inhibition model derived K_i values.

JPET Fast Forward. Published on March 22, 2005 as DOI: 10.1124/jpet.104.082826
This article has not been copyedited and formatted. The final version may differ from this version.

Discussion

Prediction of a potential DDI with CYP3A4 is challenging due to a number of in vitro and in vivo factors. Complexity of the in vitro kinetics observed for some of the CYP3A4 probes (Tang and Stearns, 2001, Houston et al., 2003), CYP3A inter-individual variability in the abundance and activity in both liver and small intestine (with the variable contribution of polymorphically expressed CYP3A5) (Lin et al., 2001, Xie et al., 2004) and overlapping substrate specificity with P-glycoprotein (Zhang and Benet, 2001) confound the straightforward prediction of a DDI.

A mechanistic approach to the analysis of in vitro homo- and heterotropic cooperative phenomena has indicated that the inclusion of CYP3A4 kinetic complexities (applying the interaction factor γ/δ ratio) into the DDI prediction strategy can provide an explanation for certain false negative and reduce the over-estimation of true positive interactions (e.g., 28-fold for ketoconazole–triazolam interaction when K_i was obtained using triazolam as a probe) (Houston and Galetin, 2003). A limitation of this approach lies in its complexity and the number of data points required for full characterization of the phenomenon observed. Therefore, we have explored the significance of multisite kinetic modelling for reliable in vitro-in vivo prediction of a range of reported in vivo interactions with azole inhibitors. For that reason, four different CYP3A4 probes, midazolam, testosterone, quinidine and nifedipine, were assessed both from the prospect of their in vitro complexities and possibility of substrate substitution in prediction of DDI potential.

Considering that testosterone and midazolam are the most widely used in vitro measures of CYP3A4 activity (Yuan et al., 2002) it is important to know the extent to which the K_i values obtained for these probes may be extrapolated to clinically used drugs (substrate substitution approach). Therefore, the success of a DDI prediction,

applying K_i values obtained for midazolam, testosterone, nifedipine and quinidine, was explored using 26 reported in vivo interactions with a range of AUCi/AUC ratios from 1.2-24 (Table 2). The predicted increase in the AUC values in the presence of the azole inhibitors was obtained by Monte Carlo simulations applying the $[I]av/K_{i,u}$ approach as this was found to be the best predictor when corresponding inhibitor-substrate pairs were investigated both in vitro and in vivo (Houston and Galetin, 2005). This was in contrast to the previous database analysis (Ito et al., 2004) where the maximum hepatic input concentration was the best surrogate for [I] for categorizing CYP inhibitors and for identifying true negative drug-drug interactions. Quinidine was assessed as an alternative and more 'pragmatic' substrate due to its hyperbolic in vitro kinetic properties and specificity towards CYP3A4 in comparison to CYP3A5 (Galetin et al., 2004).

The probes investigated differ in their in vitro complexities, from standard hyperbolic kinetics (midazolam, quinidine) to positive (testosterone) and negative cooperativity (nifedipine) (Galetin et al., 2003). In addition to in vitro differences, the substrates selected vary in their in vivo characteristics that may impact on the prediction of CYP3A4 DDI, e.g., significance of intestinal metabolism (Paine et al., 1997), involvement of P-glycoprotein (midazolam is not a substrate for this transporter in contrast to other substrates (Benet et al., 2004)) and contribution of CYP3A5 to the overall clearance (Lin et al., 2002, Huang et al., 2004).

The complexity of the inhibition models and prediction equation applied in the current study was highly dependent on the kinetic properties of the probe used. In case of midazolam and quinidine (simple hyperbolic kinetics), comparable K_i estimates were obtained by both one-site and generic two-site models and the value of the relative γ/δ ratio close to 1 (0.9-1.1) indicated the reliability of 'simple' inhibition

models for the in vitro-in vivo prediction. In contrast, the application of simple inhibition models for interactions involving substrates with positive (testosterone) or negative (nifedipine) homotropic kinetic properties is problematic and may lead to inaccurate estimation of kinetic parameters and potential DDI. However, despite complex initial kinetic analysis, a prediction equation involving the interaction factor γ/δ ratio is not necessary for cases when testosterone sigmoidicity is maintained in the presence of the inhibitor (e.g., azoles) and the simple $1+[I]/K_i$ relationship is appropriate. However, this approach is not satisfactory for nifedipine and substrates showing substrate and cooperative inhibition ($\gamma/\delta \neq 1$).

The prediction equations applied are based on the assumptions of the 'well-stirred' liver model and linear pharmacokinetics of the drug. The possibility of an interaction in the gut wall and changes in the inhibitor concentrations with the time are not incorporated and represent a limitation of this approach (Rostami and Tucker, 2004). Contrary to expectation, all four CYP3A4 probes investigated predicted 69-81% of the interactions with azoles within 2-fold of the mean in vivo value (average-fold error ranged from 0.86-1.09). However, it must be stressed that the success of the prediction is dependent upon detailed information including critical reassessment of the available in vivo information, complex multisite in vitro analysis (where necessary) and incorporation of substrate-related information on parallel elimination pathways. The contribution of other P450 enzyme (cerivastatin) or renal excretion (alprazolam, quinidine) reduced significantly the extent of DDI over-prediction (5 to 12-fold) depending on the in vitro probe used. The inhibition of the renal clearance in addition to the hepatic interaction (e.g., quinidine by itraconazole, (Kaukonen et al., 1997)) was not included, as the fraction excreted unchanged was considered to be too low (0.3) to significantly contribute to the observed interaction. Furthermore, the

majority of the studies selected (81%) were in the range of moderate to potent inhibition interactions (Fig. 1), whereas the cases of weak inhibition generally represent a problematic prediction issue (Tucker et al., 2001).

As expected, midazolam K_i values predict changes in the AUC ratio within 2-fold of in vivo values for all the interactions with benzodiazepines, consistent with the validity of substrate substitution within the same substrate subgroup (Houston and Galetin, 2003). In an analogous way, testosterone K_i gave better prediction of cyclosporine and simvastatin interactions, whereas interactions of benzodiazepines or nisoldipine were under-predicted (up 3.7-fold). A higher percentage of under-prediction was observed when the interaction potential was assessed by testosterone and nifedipine, whereas midazolam and quinidine had an equal number of under- and over-estimates (Fig. 4 A-D). Regardless of the probes investigated the interaction with tacrolimus, and in most cases atorvastatin, were over-estimated and lovastatin and simvastatin interactions were generally poorly predicted (Table 2, Fig. 5). The bias (average-fold error) observed in the predictions was not significantly different across all four CYP3A4 probes (0.86-1.08), whereas the precision (rmse) of the predictions using testosterone and nifedipine was lower in comparison to quinidine and midazolam.

A number of recent studies indicate that the clinical significance of the contribution of polymorphically-expressed CYP3A5 to the overall clearance is controversial and substrate-dependent (Floyd et al., 2003, Haufroid et al., 2004, Wong et al. 2004). In contrast to the comparable activity and kinetics observed between CYP3A4 and CYP3A5 (Williams et al., 2002, Galetin et al., 2004) this enzyme shows differential and generally less potent inhibition in comparison to CYP3A4 (Gibbs et al., 1999), indicating lower susceptibility to drug interactions even in population

groups with higher frequency of more active *CYP3A5*1* alleles (e.g., African-American). However, variable abundance and activity of CYP3A5 in both liver and intestine (Lin et al., 2002) results in the inconsistent CYP3A5 co-variation with CYP3A4 and may contribute to the variability observed in the degree of interaction. In addition to CYP3A5, the ability of both ketoconazole and itraconazole to inhibit P-glycoprotein indicates that the functional link between CYP3A4 and this transporter (in the intestine, liver or kidney) may have an impact on the degree of the interaction observed for certain CYP3A substrates (Kaukonen et al., 1997, Benet et al., 2004, Karyekar et al., 2004).

In conclusion, midazolam and quinidine provided the best assessment of a range of selected CYP3A4 drug interactions. Both substrates display hyperbolic kinetics in vitro and this adds to their 'pragmatic appeal' in the evaluation of potential DDI compared to nifedipine and testosterone. However, the current analysis has shown that the kinetic complexities of nifedipine and testosterone can be overcome by the appropriate mechanistic analysis. The success of the substrate substitution approach was highly dependent on the incorporation of additional inhibitor- (microsomal binding, depletion over incubation time) and substrate-related (cooperativity, contribution of other metabolic pathways or renal excretion) related information. The current and previous mechanistic kinetic studies (Galetin et al., 2003) support the validity of appropriate substrate substitution, and also indicate how in vitro kinetic characteristics can confound the DDI assessment. The general applicability of these findings requires further evaluation with a wider range of inhibitors.

Acknowledgements. The Authors would like to thank Dr. Ivelina Gueorguieva and Kayode Ogungbenro for their contribution on Monte Carlo simulations and variance estimates for the in vivo studies and Caroline Brown for help in testosterone experimental work.

Reference:

Armitage P, Berry G and Matthews JNS (2002) Analysing non-normal data, in *Statistical methods in medical research* pp 272-311, Blackwell Science, Oxford.

Benet LZ, Cummins CL and Wu CY (2004) Unmasking the dynamic interplay between efflux transporters and metabolic enzymes. *Int J Pharmaceut* **277**: 3-9.

Bjornsson TD, Callaghan JT, Einolf HJ, Fischer V et al. (2003) The conduct of in vitro and in vivo drug-drug interaction studies: a pharmaceutical research and manufacturers of America (PhRMA) perspective. *Drug Metab Dispos* **31**: 815-32.

Brown HS, Ito K, Galetin A and Houston JB Investigating the effects fm and ka on the prediction of in vivo drug-drug interactions from in vitro data (submitted for publication)

Egnell A-C, Eriksson C, Albertson N, Houston JB and Boyer S (2003) Generation and evaluation of CYP2C9 heteroactivation pharmacophore. *J Pharmacol Exp Ther* **307**: 878-887.

Floyd MD, Gervasini G, Masica AL, Mayo G, George Jr AL, Bhat K, Kim RB and Wilkinson GR (2003) Genotype-phenotype associations for common *CYP3A4* and *CYP3A5* variants in the basal and induced metabolism of midazolam in European- and African-American men and women. *Pharmacogenetics* **13**: 595-606.

Galetin A, Brown C, Hallifax D, Ito K and Houston JB (2004) Utility of recombinant

enzyme kinetics in prediction of human clearance – impact of variability, CYP3A5 and CYP2C19 on CYP3A4 substrates *Drug Metab Dispos* **32** 1411-1420.

Galetin A, Clarke SE and Houston JB (2003) Multisite kinetic analysis of interactions between prototypical CYP3A4 subgroup substrates: midazolam, testosterone and nifedipine. *Drug Metab Dispos* **31**: 1108-1116.

Galetin A, Clarke SE and Houston JB (2002) Quinidine and haloperidol as modifiers of CYP3A4 activity: multisite kinetic model approach. *Drug Metab Dispos* **30**: 1512-1522.

Gibbs MA, Thummel KE, Shen DD and Kunze KL (1999) Inhibition of cytochrome P-450 3A (CYP3A) in human intestinal and liver microsomes: comparison of Ki values and impact of CYP3A5 expression. *Drug Metab Dispos* **27**: 180 – 187.

Haufroid V, Mourad M, van Kerckhove V, Wawrzyniak J, de Meyer M, Eddour DC, Malaise J, Lison D, Squifflet J-P and Wallemacq P (2004) The effect of CYP3A5 and MDR1 (ABCB1) polymorphisms on cyslosporine and tacrolimus dose requirements and trough blood levels in stable renal transplant patients. *Pharmacogenetics* **14**: 147-154.

Houston JB and Galetin A (2005) Modelling atypical CYP3A4 kinetics: principles and pragmatism. *Arch Biochem Biophys* **433**:351-360.

Houston JB and Galetin A (2003) Progress towards prediction of human pharmacokinetic parameters from *in vitro* technologies. *Drug Metab Rev* **35**: 393-415.

Houston JB, Kenworthy KE and Galetin A (2003) Typical and atypical enzyme kinetics, in *Drug metabolizing enzymes: Cytochrome P450 and other enzymes in drug discovery and development* (Fisher M, Lee J, Obach S, eds) pp 211-254, Fontis Media, Lausanne.

Huang W, Lin YS, McConn II DJ, Calamia JC, Totah RA, Isoherranen N, Glodowski M and Thummel KE (2004) Evidence of significant contribution from CYP3A5 to hepatic drug metabolism. *Drug Metab Dispos* **32**: 1434-1445.

Hutzler JM, Wienkers LC, Wahlstrom JL, Carlson TJ and Tracy TS (2003) Activation of cytochrome P450 2C9-mediated metabolism: mechanistic evidence in support of kinetic observations. *Arch Biochem Biophys* **410**: 16-24.

Isoherranen N, Kunze KL, Allen KE, Nelson WL and Thummel KE (2004) Role of itraconazole metabolites in CYP3A4 inhibition. *Drug Metab Dispos* **32**: 1121-1131.

Ito K, Brown HS and Houston JB (2004) Database analyses for the prediction of in vivo drug-drug interactions from in vitro data. *Br J Clin Pharmacol* **57**: 473-486 and Erratum *Br J Clin Pharmacol* **58**: 565-568.

Karyekar CS, Eddington ND, Briglia A, Gubbins PO and Dowling TC (2004) Renal interaction between itraconazole and cimetidine. *J Clin Pharmacol* **44**: 919-927.

Kaukonen K-M, Olkkola KT and Neuvonen PJ (1997) Itraconazole increases plasma concentrations of quinidine. *Clin Pharmacol Ther* **62**: 510-17.

Kenworthy K, Bloomer JC, Clarke SE and Houston JB (1999) CYP3A4 drug interactions: correlation of ten *in vitro* probe substrates. *Br J Clin Pharmacol* **48**: 716-727.

Korzekwa K (2002) In vitro enzyme kinetics applied to drug-metabolizing enzymes. in *Drug-drug interactions* (Rodrigues AD, eds) pp 33-54, Marcel Dekker Inc., New York.

Lin YS, Dowling ALS, Quigley SD, Farin FM, Zhang J, Lamba J, Schuetz EG and Thummel KE (2002) Co-regulation of CYP3A4 and CYP3A5 and contribution to hepatic and intestinal metabolism of midazolam. *Mol Pharmacol* **62**: 162-172.

Nestorov I, Gueorguieva I, Jones H, Houston JB and Rowland M (2002) Incorporating measures of variability and uncertainty into the prediction of in vivo hepatic clearance from in vitro data. *Drug Metab Dispos* **30**: 276-82.

Obach RS, Baxter JG, Liston TE, Silber BM, Jones BC, MacIntyre F, Rance DJ and Wastall P (1997) The prediction of human pharmacokinetic parameters from preclinical and in vitro metabolism data. *J Pharmacol Exp Ther* **283**: 46-58.

Paine MF, Khalighi M, Fisher JM, Shen DD,Kunze KL, Marsh CL, Perkins JD and Thummel KE (1997) Characterization of interintestinal and intraintestinal variations in human CYP3A-dependent metabolism. *J Pharmacol Exp Ther* **283**: 1552-1562.

Rostami-Hodjegan A and Tucker GT (2004) '*In silico'* simulations to assess the 'in vivo' consequences of 'in vitro' metabolic drug-drug interactions. *Drug Discovery Today* **1**: 441-448.

Rowland M and Matin SB (1973) Kinetics of drug-drug interactions. *J Pharmacokinet Biopharm* 1: 553-567.

Segel IH (1975*) Enzyme Kinetics: Behaviour and Analysis of Rapid Equilibrium and Steady State enzyme Systems*. Wiley & Sons Inc, New York.

Sheiner LB and Beal SL (1981) Some suggestions for measuring predictive performance. *J Pharmacokinet Biopharm* **9**: 503-512.

Stresser DM, Blanchard AP, Turner SD, Erve JCL, Dandeneau AA, Miller VP and Crespi CL (2000) Substrate-dependent modulation of CYP3A4 catalytic activity: analysis of 27 test compounds with four fluorometric substrates. *Drug Metab Dispos* **28**: 1440-1448.

Tang W and Stearns RA (2001) Heterotropic cooperativity of cytochrome P450 3A4 and potential drug-drug interactions. *Curr Drug Metab* **2**: 185-198.

Tucker GT, Houston JB and Huang, S-M (2001) Optimizing drug development: Strategies to assess drug metabolism/transporter interaction potential - toward a consensus. *Clin Pharmacol Ther* **70**: 103-114.

Uchaipichat V, Mackenzie PI, Guo X-H, Gardner-Stephen D, Galetin A, Houston JB and Miners JO (2004) Human UDP-glucuronosyltransferases: Isoform selectivity and kinetics of 4-methylumbelliferone and 1-naphthol glucuronidation, effects of organic solvents, and inhibition by diclofenac and probenecid *Drug Metab Dispos* **32**: 413-423.

Varhe A, Olkkola KT and Neuvonen PJ (1994) Oral triazolam is potentially hazardous to patients receiving systemic antimycotics ketoconazole and itraconazole. *Clin Pharmacol Ther* **56**: 601-7

Williams JA, Ring BJ, Cantrell VE, Jones DR, Eckstein J, Ruterbories K, Hamman MA, Hall SD and Wrighton SA (2002) Comparative metabolic capabilities of CYP3A4, CYP3A5 and CYP3A7. *Drug Metab Dispos* **30**: 883-891.

Wong M, Balleine RL, Collins M, Liddle C, Clarke CL, Gurney H (2004) CYP3A5 genotype and midazolam clearance in Australian patients receiving chemotherapy. *Clin Pharmacol Ther* **14**: 471-478.

Xie H-G, Wood AJJ, Kim RB, Stein CM and Wilkinson GR (2004) Genetic variability in CYP3A5 and its possible consequences. *Pharmacogenomics* **5**: 243-272.

Yuan R, Madani S, Wei X-X, Reynolds K and Huang S-M (2002) Evaluation of cytochrome P450 probe substrates commonly used by the pharmaceutical industry to study in vitro drug interactions. *Drug Metab Dispos* **30**: 1311-19.

Zhang Y and Benet LZ (2001) The gut as a barrier to drug absorption. *Clin Pharmacokinet* **40**: 159-168.

FOOTNOTES

Financial support for this project was provided by the following Centre for Applied Pharmacokinetic Research (CAPkR) Consortium members: Bristol Myers-Squibb, Eli Lilly, GlaxoSmithKline, Novartis, Pfizer, F. Hoffmann La Roche and Servier.

Address correspondence to: Dr A. Galetin, School of Pharmacy and Pharmaceutical Sciences, University of Manchester, Oxford Rd, Manchester, M13 9PL, UK

JPET Fast Forward. Published on March 22, 2005 as DOI: 10.1124/jpet.104.082826
This article has not been copyedited and formatted. The final version may differ from this version.

Legends for Figures

Fig. 1. Classification of the 26 CYP3A4 in vivo studies investigated according to Bjornsson et al. (2003) indicated that 19% of studies were cases of weak inhibition (□, AUCi/AUC < 2), 30% moderate (▭, 2 < AUCi/AUC < 5) and the remainder (50%) were potent (■, AUCi/AUC > 5). The order of in vivo studies shown corresponds to the listing in Table 2.

Fig. 2. Lack of association between the K_i and γ/δ ratio obtained for the interaction of nifedipine with azole inhibitors.

Fig. 3. The effect of increasing concentrations of azoles on the metabolism of midazolam (A), quinidine (B), testosterone (C) and nifedipine (D) in human liver microsomes. A: midazolam (2.5-50 μM), B: quinidine (25-250 μM), C: testosterone (5-200 μM) and D: nifedipine (2.5-100 μM). Data points represent the mean of duplicate determinations. The lines represent the simultaneous fit to the corresponding models defined in the Methods at ketoconazole concentrations of 0, 0.03, 0.1, 0.3 and 1μM (for midazolam and quinidine) or itraconazole concentrations of 0, 0.03, 0.3, 1 and 3 μM (testosterone) and 0, 0.1, 0.3, 1 and 3 μM (nifedipine).

Fig. 4. Comparison of mean AUCi/AUC ratios predicted by Monte Carlo simulations applying $[I]av/K_{i,u}$ using K_i values for midazolam (A), testosterone (B), quinidine (C) and nifedipine (D) and AUC ratios observed in vivo for 26 DDI where ■ represents ketoconazole (8), △ itraconazole (12) and ● fluconazole (6). The solid line

represents line of unity, whereas dashed lines represent the 2-fold limit in prediction accuracy.

Fig. 5. Evaluation of substrate substitution in the prediction of 26 observed CYP3A4 drug interactions using midazolam, testosterone, quinidine and nifedipine as in vitro probes. Studies are divided into few groups – benzodiazepines, cyclosporine and tacrolimus, nifedipine and felodipine, and statins.

TABLE 1

K_i (μM) estimates for ketoconazole, itraconazole and fluconazole obtained in human liver pooled microsomes using midazolam, testosterone, quinidine and nifedipine as probes

Probe substrate	**Inhibitors**		
	Ketoconazole	Itraconazole	Fluconazole
Midazolam	0.059 ± 0.003	0.50 ± 0.04	11.9 ± 0.9
Testosterone[a]	0.17 ± 0.01	0.23 ± 0.02	27.6 ± 2.1
Quinidine	0.053 ± 0.004	0.32 ± 0.08	13 ± 1
Nifedipine[b]	0.52 ± 0.19	3.12 ± 0.71	86 ± 3

K_i values for ketoconazole and itraconazole were corrected for the microsomal fraction unbound (0.71 and 0.056, respectively at the protein concentration used in the study (0.25 mg/mL).

[a] Three-site kinetic model defined in Galetin et al., 2002, α = 0.09-0.13

[b] γ/δ ratio is 0.2, 0.3 and 0.67 for ketoconazole, itraconazole and fluconazole, respectively

JPET Fast Forward. Published on March 22, 2005 as DOI: 10.1124/jpet.104.082826
This article has not been copyedited and formatted. The final version may differ from this version.

TABLE 2

List of observed in vivo and predicted AUCi/AUC ratios for 26 drug interactions with azole inhibitors using midazolam, testosterone, quinidine and nifedipine as probes

Interaction	Mean AUCi/AUC in vivo	Mean AUCi/AUC predicted				fm
		Midazolam	Testosterone	Quinidine	Nifedipine	
Ketoconazole – midazolam[1]	15.9	14.1	6.5	14.4	15.7	0.99
Ketoconazole – triazolam[2]	9.2	12.5	6.2	12.7	13.7	0.98
Ketoconazole – triazolam[3]	13.7	12.5	6.2	12.7	13.7	0.98
Ketoconazole – triazolam[4]	9.2	12.5	6.2	12.7	13.7	0.98
Ketoconazole – alprazolam[3]	3.98	4.0	3.2	4.0	4.1	0.80
Ketoconazole – cyclosporine[5]	4.9	16.3	6.9	16.6	18.4	1.00
Ketoconazole – nisoldipine[6]	24.4	14.1	6.5	14.4	15.7	0.99
Ketoconazole – tacrolimus[7]	1.2	10.6	6.5	14.4	15.7	0.99
Itraconazole – quinidine[8]	2.4	3.1	3.4	3.2	2.9	0.76
Itraconazole – felodipine[9]	6.3	8.0	12.5	9.3	6.5	0.99
Itraconazole – simvastatin[10]	18.4	8.0	12.5	9.3	6.5	0.99
Itraconazole – alprazolam[11]	2.7	3.4	3.9	3.6	3.2	0.80
Itraconazole – midazolam[12]	5.7	5.5	7.1	6.3	3.2	0.99
Itraconazole – midazolam[13]	6.4	8.0	12.5	9.3	6.5	0.99
Itraconazole – midazolam[1]	10.8	11.6	20.3	14.6	13.4	0.99
Itraconazole – triazolam[2]	10.5	7.5	11.2	8.5	6.2	0.98
Itraconazole – atorvastatin[14]	3.6	8.0	12.2	9.3	6.5	0.99
Itraconazole – cerivastatin[15]	1.15	1.5	1.5	1.5	1.5	0.37
Itraconazole – lovastatin[16]	8.6	3.9	4.6	4.3	2.7	0.90
Itraconazole – lovastatin[17]	21.6	5.2	6.1	5.3	4.3	0.90
Fluconazole – midazolam[18]	3.6	2.8	1.8	2.6	1.15	0.99
Fluconazole – triazolam[19]	1.6	1.5	1.2	1.4	1.02	0.98
Fluconazole – triazolam[20]	2.3	1.9	1.4	1.8	1.05	0.98
Fluconazole – triazolam[19]	4.4	2.7	1.8	2.6	1.15	0.98
Fluconazole – cyclosporine[21]	1.8	2.8	1.8	2.6	1.15	1.00
Fluconazole – rifabutin[22]	1.8	2.4	1.7	2.3	1.13	0.90

[1]Olkkola et al. (1994) *Clin Pharmacol Ther* **55**:481-5; [2]Varhe et al. (1994) *Clin Pharmacol Ther* **56**:601-7; [3]Greenblatt et al. (1998) *Clin Pharmacol Ther* **64**:237-47; [4] von Moltke et al. (1996) *J Pharmacol Exp Ther* **276**:370-9; [5]Gomez et al. (1995) *Clin Pharmacol Ther* **58** :15-19, Foradori et al. (1998) *Transplant Proc* **30**:1685-7; [6]Heinig et al. (1999) *Eur J Clin Pharmacol* **55**:57-60; [7]Floren et al. (1997) *Clin Pharmacol Ther* **62**:41-9; [8] Kaukonen et al. (1997) *Clin Pharmacol Ther* **62**:510-7; [9] Jalava et al. (1997) *Clin Pharmacol Ther* **61**:410-5; [10] Neuvonen et al. (1998) *Clin Pharmacol Ther* **63**:332-41; [11] Yasui et al. (1998) *Psychopharmacology* **139**:269-73; [12] Ahonen et al. (1995) *Br J Clin Pharmacol* **40**:270-2; [13] Backman et al. (1998) *Eur J Clin Pharmacol* **54**:53-8, Olkkola et al. (1996) Anesth Analg **82**:511-6; [14] Kantola et al. (1998) *Clin Pharmacol Ther* **64**:58-65; [15] Kantola et al. (1999) *Eur J Clin Pharmacol* **54**:851-5; [16] Kivisto et al. (1998) *Br J Clin Pharmacol* **46**:49-53; [17] Neuvonen & Jalava (1996) *Clin Pharmacol Ther* **60**:54-61; [18] Olkkola et al. (1996) *Anesth Analg* **82**:511-6; [19] Varhe et al. (1996) *Br J Clin Pharmacol* **42**:465-70; [20] Varhe et al. (1996) *Br J Clin Pharmacol* **41**:319-23; [21] Canafax et al. (1991) *Transplantation* **51**:1014-8; [22] Trapnell et al. (1996) *Ann Intern Med* **124**:573-6.

Figure 1

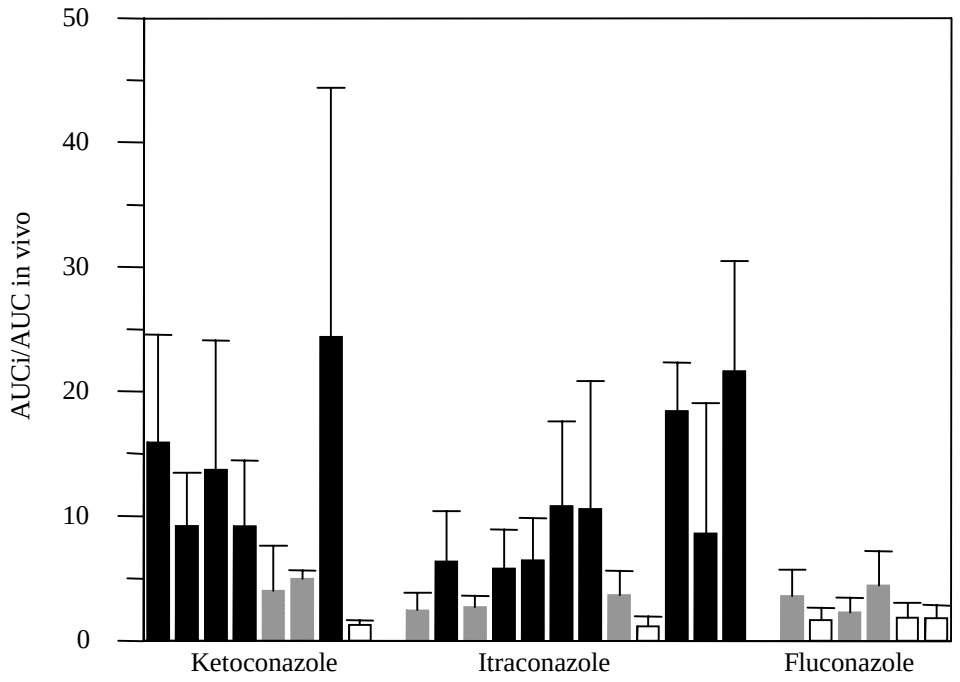

Figure 2

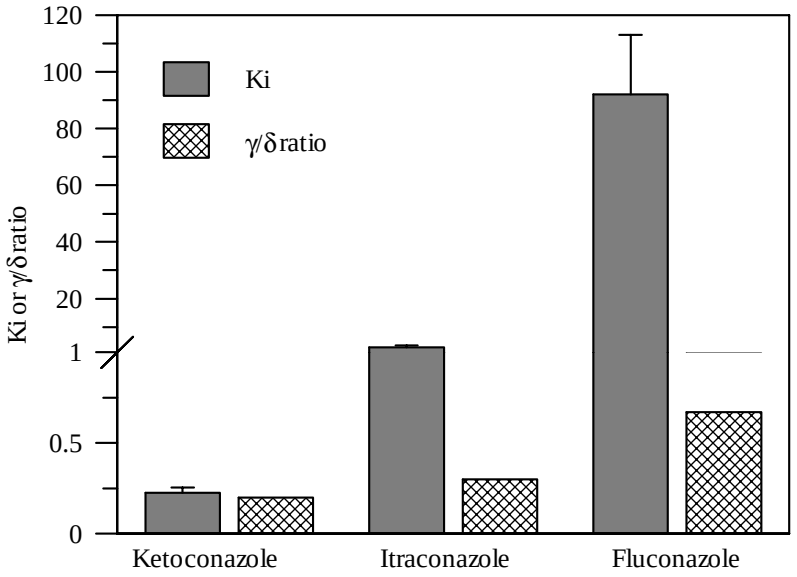

Figure 3

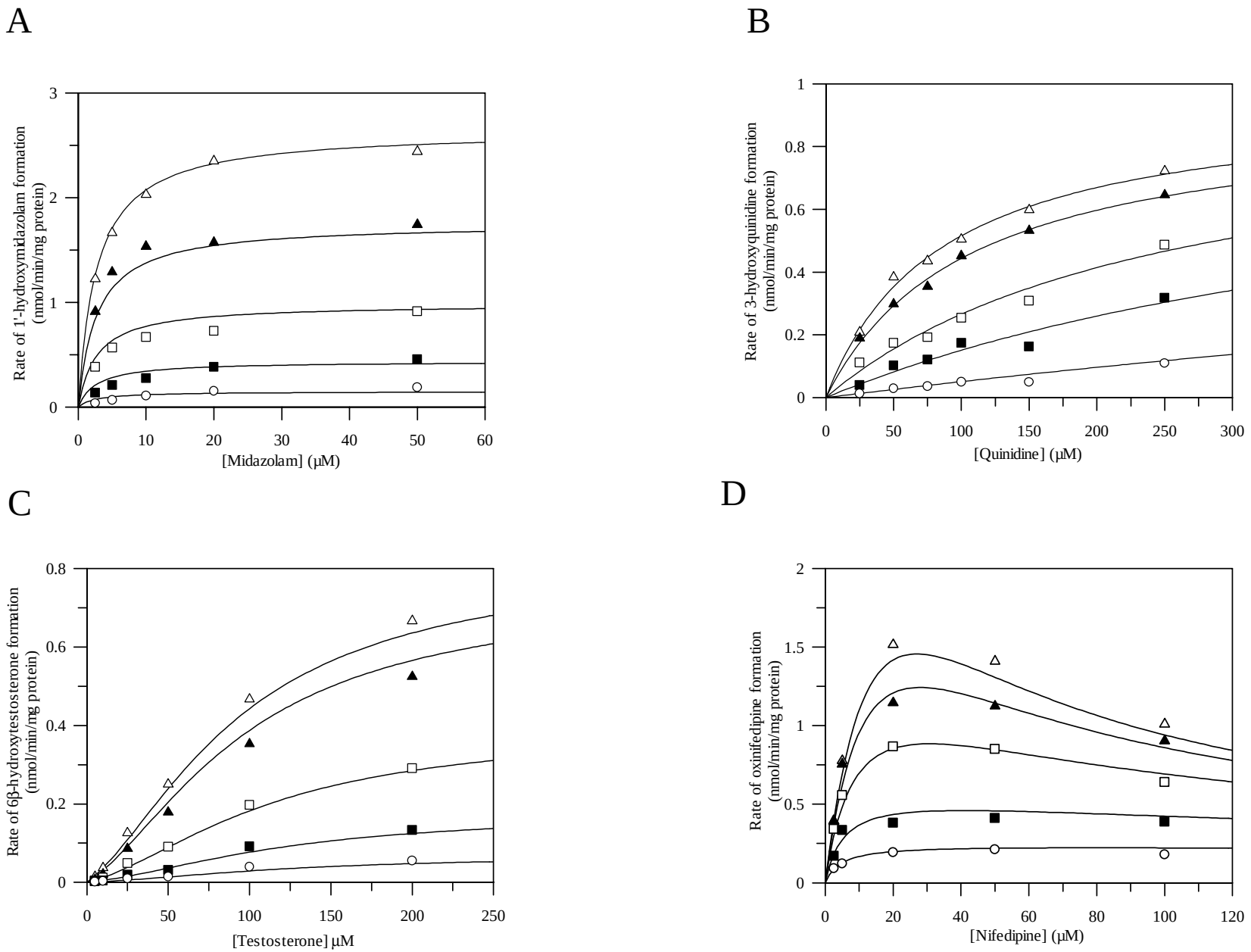

Figure 4

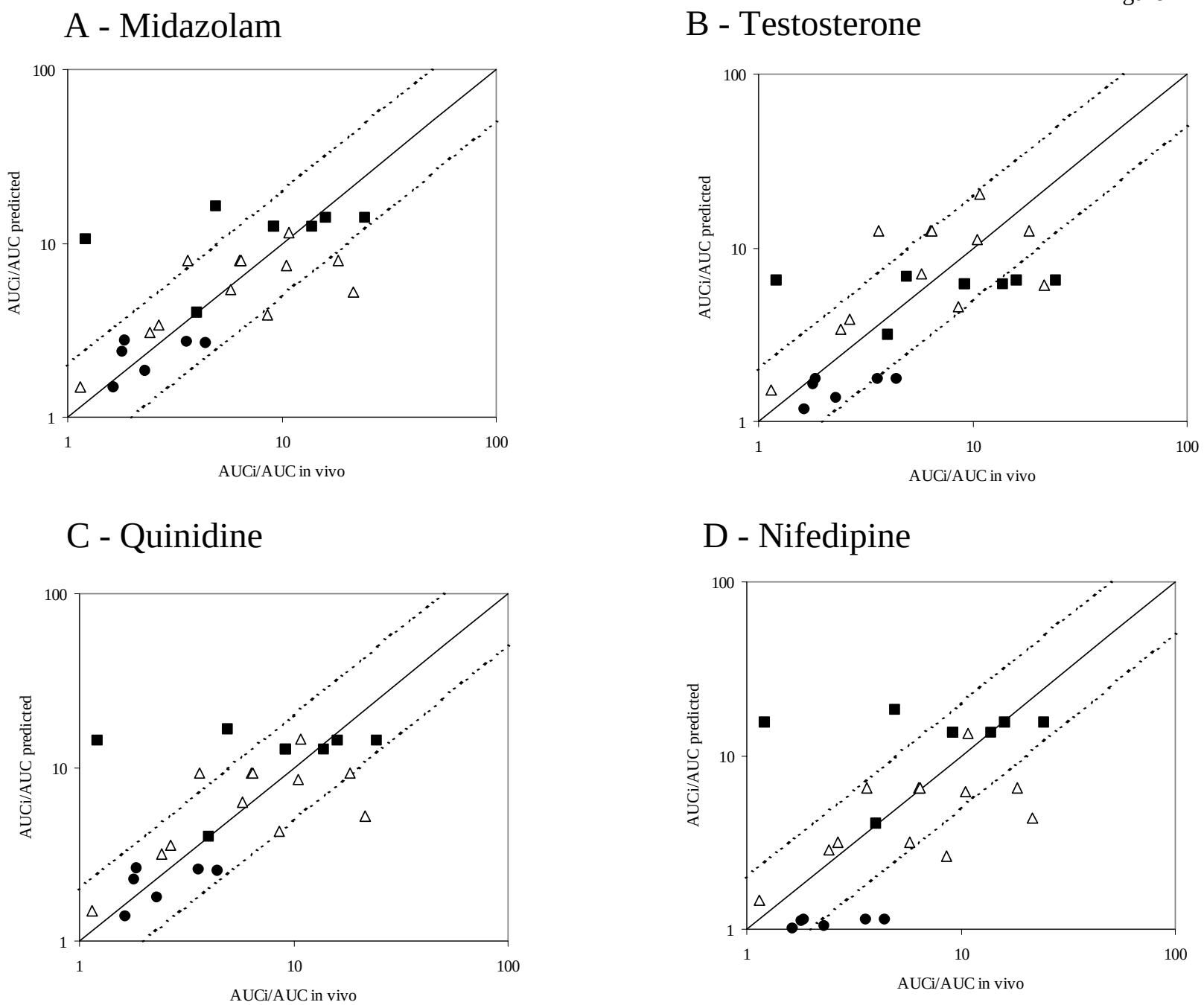

Figure 5

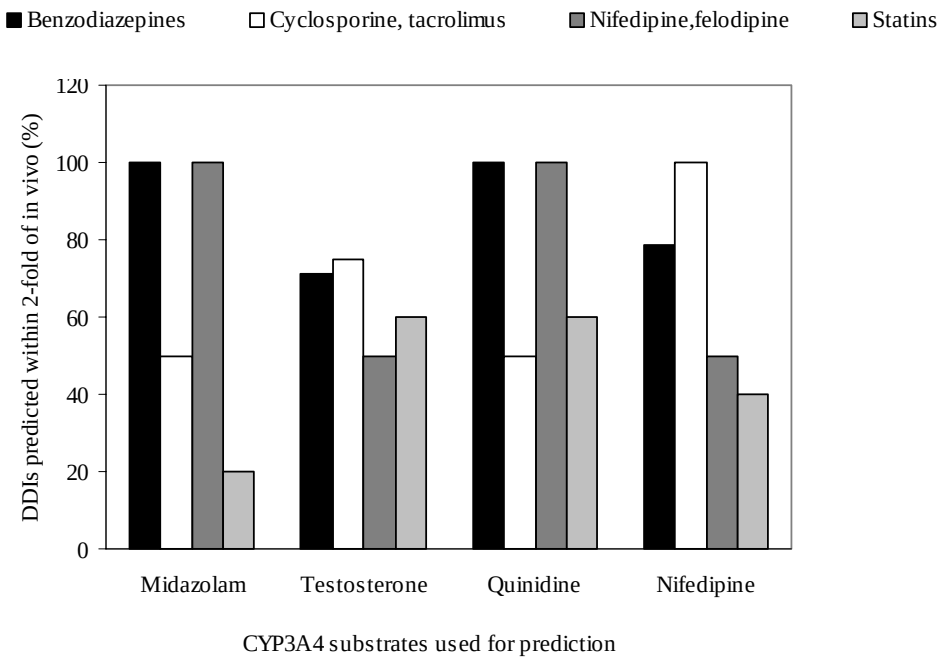

JPET Fast Forward. Published on March 22, 2005 as DOI: 10.1124/jpet.104.082826
This article has not been copyedited and formatted. The final version may differ from this version.

APPENDIX

A. In vitro-in vivo relationship for substrates showing negative homotropic behaviour (e.g., nifedipine) and cooperative inhibition

In the case of substrate inhibition the decrease in the rate of product formation (K_p) from a two-substrate bound complex is described by the interaction factor $\beta<1$. The kinetic model defined by equation 7 incorporates sequential binding of substrate molecules, i.e. the 'substrate inhibition site' cannot be occupied until the active site is filled and the second site may be independent from the active site (Houston et al., 2003). The final form of the equation is obtained after multiplying both the numerator and denominator by K_s.

$$\frac{v}{Vmax} = \frac{\frac{[S]}{Ks} + \frac{\beta[S]^2}{Ks^2}}{1 + \frac{[S]}{Ks} + \frac{[S]^2}{Ks^2}} = \frac{[S]\left(1+\frac{\beta[S]}{Ks}\right)}{Ks + [S]\left(1+\frac{[S]}{Ks}\right)} \qquad (7)$$

The alterations in the product formation due to the presence of an inhibitor molecule at the active site are defined by the interaction factor γ. In cases when substrate inhibition phenomenon remains the effect of a modifier is analogous to the binding of a second substrate molecule and γ is comparable to β. At high concentrations of substrate and inhibitor the profile changes to a hyperbolic curve due to dominance of the non-productive S(EI) complex (Galetin et al., 2003). The following equation has been rearranged multiplying the initial equation by K_s, analogous to the case with no inhibitor.

$$\frac{v}{Vmax} = \frac{\frac{[S]}{Ks} + \frac{\beta[S]^2}{Ks^2} + \frac{\gamma[S][I]}{\delta KsKi}}{1 + \frac{[S]}{Ks} + \frac{[S]^2}{Ks^2} + \frac{2[S][I]}{\delta KsKi} + \frac{2[I]}{Ki} + \frac{[I]^2}{Ki^2}} = \frac{[S]\left(1+\frac{\beta[S]}{Ks}+\frac{\gamma[I]}{\delta Ki}\right)}{Ks\left(1+\frac{2[I]}{Ki}+\frac{[I]^2}{Ki^2}\right)+[S]\left(1+\frac{[S]}{Ks}+\frac{2[I]}{\delta Ki}\right)} \qquad (8)$$

JPET Fast Forward. Published on March 22, 2005 as DOI: 10.1124/jpet.104.082826
This article has not been copyedited and formatted. The final version may differ from this version.

Similar to single-site models, rapid equilibrium and steady state principles have been used to assess the importance of cooperativity and predict changes in the in vivo plasma concentration-time profile from CYP3A4 in vitro data. The first order kinetics ([S] <<K_s) assumption allows the simplification of the ratio of equations 7 and 8 and derivation of the two-site prediction equation in a form presented in the equation 9.

$$\frac{AUCi}{AUC} = \frac{CL}{CL_i} = \frac{Ks\left(1+\frac{[I]}{Ki}\right)^2 + [S]\left(1+\frac{[S]}{Ks}+\frac{2[I]}{\delta Ki}\right)}{Ks\left(1+\frac{\beta[S]}{Ks}+\frac{\gamma[I]}{\delta Ki}\right)} = \frac{\left(1+\frac{[I]}{Ki}\right)^2}{1+\frac{\gamma[I]}{\delta Ki}} \qquad (9)$$

In addition to $[I]/K_i$ ratio, this prediction equation also incorporates changes in the catalytic efficacy (γ) and binding affinity (δ) in the presence of the inhibitor. In cases when γ/δ =1, two-site prediction equation (eq. 9) is reduced to the simple relationship $1+[I]/K_i$.

B. In vitro-in vivo relationship for substrates showing positive homotropic behaviour (e.g., testosterone)

Autoactivation is defined by the following two-site kinetic model (Houston et al., 2003), assuming that β=2 (V_{max} is equivalent to $2K_p[E]_t$, where $[E]_t$ is the total enzyme concentration (Segel, 1975)), where $\alpha < 1$ defines the change in the dissociation constant K_s.

$$\frac{v}{Vmax} = \frac{\frac{[S]}{Ks} + \frac{[S]^2}{\alpha Ks^2}}{1 + \frac{2[S]}{Ks} + \frac{[S]^2}{\alpha Ks^2}} = \frac{[S]\left(1+\frac{[S]}{\alpha Ks}\right)}{Ks + [S]\left(2+\frac{[S]}{\alpha Ks}\right)} \qquad (10)$$

JPET Fast Forward. Published on March 22, 2005 as DOI: 10.1124/jpet.104.082826
This article has not been copyedited and formatted. The final version may differ from this version.

In the presence of increasing concentrations of the modifier, the interaction between two substrate molecules, and the sigmoidal properties of the substrate, are unaffected suggesting that the inhibitor acts at a distinct effector site. Inhibition is not consistent with a competitive type, as the modifier causes changes in V_{max}, rather than changes in the substrate binding constant K_s (equation 11). Similar to the equations described under A, the final form of equations 10 and 11 has been obtained by multiplying numerator and denominator by K_s.

$$\frac{v}{Vmax} = \frac{\frac{[S]}{Ks} + \frac{[S]^2}{\alpha Ks^2}}{1 + \frac{2[S]}{Ks} + \frac{[S]^2}{\alpha Ks^2} + \frac{[I]}{Ki} + \frac{2[S][I]}{KsKi} + \frac{[S]^2[I]}{\alpha Ks^2 Ki}} = \frac{[S]\left(1 + \frac{[S]}{\alpha Ks}\right)}{\left(Ks + 2[S] + \frac{[S]^2}{\alpha Ks^2}\right)\left(1 + \frac{[I]}{Ki}\right)} \qquad (11)$$

The AUCi/AUC prediction equation is derived as a ratio of equations 10 and 11 and under the same first order kinetics assumptions as for the cases of negative homotropic behaviour. Due to the nature of the interaction (sigmoidicity is maintained in the presence of the inhibitor) DDI prediction equation involving the interaction factors (eq. 9) is not necessary and the simple $1+[I]/K_i$ relationship is appropriate (equation 12).

$$\frac{AUCi}{AUC} = \frac{CL}{CL_i} = 1 + [I]/Ki \qquad (12)$$